Excitation Stimuli For Simultaneous Deconvolution

Sunil Bharitkar, Ema Souza-Blanes, Pascal Brunet
DMS-Audio Lab, Samsung Research America
s.bharitkar@samsung.com

***Abstract*—In this paper, we present a new technique to deconvolve multiple loudspeaker-room impulse responses from a single time-domain measurement. The time-domain measurement is obtained by exciting all loudspeakers simultaneously with a stimulus designed by incorporating a Bayesian optimization algorithm. Specifically, the parameters of the stimuli (duration and right-circular shift values) are optimized by the algorithm by minimizing a *time-domain error* between the actual impulse responses and the deconvolved responses over a training dataset. The paper compares, objectively and subjectively, three well-known stimuli used for home and cinema loudspeaker calibration, showing that the log-sweep performs the best in terms of the lowest error and yields the highest preference as a short-duration stimulus for in-room calibration[1].**

***Index Terms*—Deconvolution, room impulse response, stimulus, Bayes optimization, log-sweep, multitone, pink noise, maximum-length sequence**

I. Introduction

Loudspeaker-room calibration is important for delivering high-quality immersive spatial audio in homes, cinemas, and automobiles. The calibration involves first acquiring a loudspeaker-room impulse response from a loudspeaker to a listening position. Subsequently, a DSP processor can implement appropriate time delay, loudness/level, and spectral equalization based on the measured room impulse response. The state-of-the-art (SOTA) approach involves deconvolving the response $h_{i,j}(n)$, from an in-room measurement at a microphone position j, by exciting a loudspeaker i with an excitation stimulus ([5]-[18]), and then deconvolving that loudspeaker-room impulse response before proceeding sequentially to the next loudspeaker. Huang [20] provides a tutorial on blind and non-blind MIMO system identification.

The popular stimuli for acquiring room responses are pink noise which is a standard for cinema calibration [19], maximum length sequence (MLS) due to its well-understood mathematical properties [33], and log-sweep due to its advantages over various stimuli [21]. Prawda *et al.* [22] presents a technique for improving the robustness of exponential sweep measurements in the presence of impulsive and non-stationary noise.

The disadvantage of sequential measurements becomes apparent when the number of loudspeakers and positions increases, as the time required to deconvolve room responses from all loudspeakers will increase. Furthermore, repeated measurements for increasing the SNR will add to the measurement and, thereby, calibration time. Newer approaches to address this limitation include the work presented by Majdak *et al.* [23], and Weinzierl *et al.* [24] based on interleaving or partial overlapping sweep stimuli. Antweiler *et al.* [25] present an adaptive filtering technique to perform multiple-input single-output (MISO) system identification using perfect sequences [26], which satisfy orthogonality, are odd-symmetric in phase, and have a constant magnitude spectrum [27]. Nakahara *et al.* [28] presents a short-duration sweep that is optimized, for single-channel deconvolution, by ensuring constant normalized noise power in the analysis frequency bands of the magnitude response. Bharitkar [3] presents a technique (as depicted in Fig. 1) for simultaneous deconvolution by exciting all loudspeakers *simultaneously*. The log-sweep stimulus was optimized by computing the *log spectral distortion metric*, between the actual magnitude response and the estimated response, as a function of duration and circular shift using Bayesian optimization. The deconvolution is validated in the real-world [2] in different acoustical environments with varying signal-to-noise ratio (SNR).

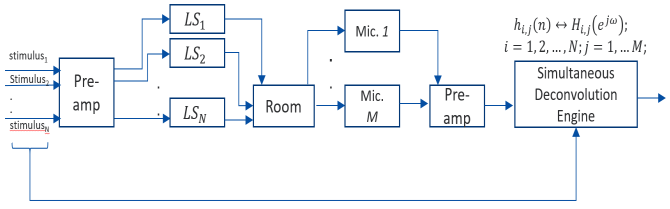

Fig. 1: Presented approach of simultaneous room response, $h_{i,j}(n)$, deconvolution for all loudspeakers ($LS_i; i = 1,2,...,N$) and microphone position j.

The key advancements in this paper are: (i) using stimuli that are not constrained to be PSEQ (flat magnitude spectrum, odd-symmetric phase, or orthogonal), (ii) incorporating impulse response error minimization in the Bayesian optimization enabling time-delay estimation and dereverberation, (iii) creating a large dataset comprising two room response databases, with interpretability, for use in developing the algorithm, (iv) Bayesian optimization and comparisons between three popular excitation signals including the MLS (white), multitone (pink), and log-sweep for simultaneous deconvolution, (v) objectively comparing the three stimuli using statistical analysis on the test set for generalization ability, and (vi) listening tests comparing the optimized 11-channel stimuli when delivered to all 11-loudspeakers at the same time in a 7.1.4 (11-loudspeaker and ignoring subwoofer) setup. Section II summarizes the properties of the three excitation stimuli

[1]The authors thank Samsung Electronics and Samsung Research America for supporting this research

used in this paper, the simultaneous deconvolution basics and the dataset creation approach. Section III presents the Bayesian algorithm for optimizing the excitation stimuli parameters using the impulse responses for training and testing. Section IV presents objective results on the modeling performance with each stimulus over a test set as well as subjective test results in Samsung's reference ITU setup room. Section V concludes/summarizes the paper.

II. Excitation Stimulus

A. Multitone (pink spectrum)

As an input signal for system identification, the multitone [29]-[32] with a specific amplitude, frequency, and random phase distribution is expressed as $u(t) = \sum_{k=-N/2+1}^{N/2-1} U_k e^{j\omega_k t}$, where the phases $\angle U_k$ are random and uniformly distributed on $[0, 2\pi[$. This phase distribution ensures a signal with random values and an amplitude distribution that tends asymptotically to a Gaussian law when $N \to \infty$. The amplitude spectrum $|U_k|$ in this paper is pink, with the signal being zero mean ($|U_0| = 0$).

B. Maximum-length sequence

A Maximum-Length Sequence (MLS) [33], is a periodic two-level signal of length $P = 2^L - 1$, where L is an integer, and P the periodicity. Correlation techniques or the Fast Hadamard Transform extracts the impulse response. Maximum-Length Sequences have several attractive properties, including that the autocorrelation is an impulse (with a white spectrum) except for a DC offset. The circular correlation for lag k with an MLS signal satisfies,

$$r_{x,x}(k) = \delta(k) - \frac{1}{L+1} \tag{1}$$

C. Logarithmic Sine-sweep

In the case of an exponential sweep, [34], assuming ω_1 and ω_2 being the start and end frequencies, with a total duration of T_{log} seconds, the logarithmic sweep signal $x(t)$ is

$$x(t) = \sin\left(\frac{\omega_1 T_{\log}}{\log \frac{\omega_2}{\omega_1}} \left(e^{\frac{t}{T_{\log}} \log\left(\frac{\omega_2}{\omega_1}\right)} - 1\right)\right) \tag{2}$$

whereas the discrete-time equivalent is $\mathbf{x}_1(n) = (x(n), x(n-1), x(n-2), \ldots, x(n-(P-1)))^T$, T represents the vector transpose and $P = T_{log}/T_s$ in samples[2],[3].

D. Simultaneous Deconvolution

The measurement (recording), assuming noiseless condition, is a linear convolution sum between the loudspeaker-room response $\mathbf{h}_i$ and the stimuli $\mathbf{x}_i(n)$,

$$\mathbf{y}(n) = \sum_{i=1}^{N=11} \mathbf{x}_i(n) \circledast \mathbf{h}_i \tag{3}$$

with

$$\mathbf{x}_1(n) = [x(n), x(n-1), \ldots, x(n-P+1)]^T \tag{4}$$
$$\mathbf{x}_i(n) = [x(<n-(i-1)M>_P), x(<n-(i-1)M-1>_P), \ldots, x(<n-(i-1)M-P+1>_P)]^T; \quad (i = 2, \ldots, 11)$$

with $<m>_P = m$ modulo P, and $\mathbf{h}_i = [h_i(1), h_i(2), \ldots, h_i(K)]^T$ is a K-length impulse response. Bharitkar [3] presents a fast implementation involving computing the cross-spectrum between the measurement and excitation stimuli and the auto-spectrum of the excitation stimuli (appropriately circularly-shifted) to deconvolve room responses from loudspeakers excited simultaneously. Specifically,

$$\begin{aligned} S_{\mathbf{x}_j,\mathbf{x}_j}(e^{j\omega}) &= \mathscr{F}\{\mathbf{x}_j(n)\}\mathscr{F}\{\mathbf{x}_j(n)\}^* \\ S_{\mathbf{x}_j,\mathbf{y}}(e^{j\omega}) &= \mathscr{F}\{\rho_{(\mathbf{x}_j(n),\mathbf{y}(n))}\} = \mathscr{F}\{\mathbf{x}_j(n)\}\mathscr{F}\{\mathbf{y}(n)\}^* \\ \hat{H}_j(e^{j\omega})) &= \frac{S_{\mathbf{x}_j,\mathbf{y}}(e^{j\omega})}{S_{\mathbf{x}_j,\mathbf{x}_j}(e^{j\omega})} \\ \hat{\mathbf{h}}_j &= \mathscr{F}^{-1}\{\hat{H}_j(e^{j\omega})\} \end{aligned} \tag{5}$$

E. Dataset Creation

The room impulse responses used in this paper are from MARDY [35][4] and MeshRiR [36][5] databases. The MARDY database has 72 loudspeaker-room responses obtained in a variable acoustics room with a Genelec 1029A loudspeaker. In contrast, MeshRiR has 14112 responses from a room with an array of 32 loudspeakers and a rectangular grid of 21×21 microphone positions[6]. Based on an augmented dataset (created by combining both databases), the number of 11-channel responses available for simulations is binomial $\binom{14112+72}{11} \approx 10^{38}$.

The distribution of the responses from both databases is shown in Fig. 2(a) with the *t-SNE* algorithm [37], which maps multidimensional distance into two- or three-dimensional distances for visualization after minimizing the Kullback-Leibler divergence loss. The spread (cluster size) for each class (database) is large, with large distances between responses from the databases. Specifically, Fig. 2(c) shows three responses, with two responses from MARDY (top two subplots) being temporally similar (albeit subtle differences in the relative amplitudes and delay). Figure 2(c) bottom subplot shows an example response from MeshRiR and is highly dissimilar to the MARDY responses (top two subplots). Accordingly, this dissimilarity maps to the 3D representation of these three responses in Fig. 2(b), where similar responses are closer than dissimilar ones. In the context of the convolution sum, the data augmentation between databases provides a large diversity in the measurement signal arising from random interleaving of the impulse responses for each 11-channel set used in the training and test portions of the dataset. Specifically, an 11-channel impulse response set used during training or testing could contain individual responses from both databases (or either database).

[2] $T_s = 1/f_s = 1/48000$ (s), and f_s is the sampling frequency

[3] $T_{\text{stimuli}} = P_{\text{stimuli}}/48000$, where stimuli are either log-sweep, MLS, or multitone-pink

[4] https://www.commsp.ee.ic.ac.uk/ sap/

[5] https://github.com/sh01k/MeshRIR

[6] The number of responses is $32 \times 21 \times 21 = 14112$

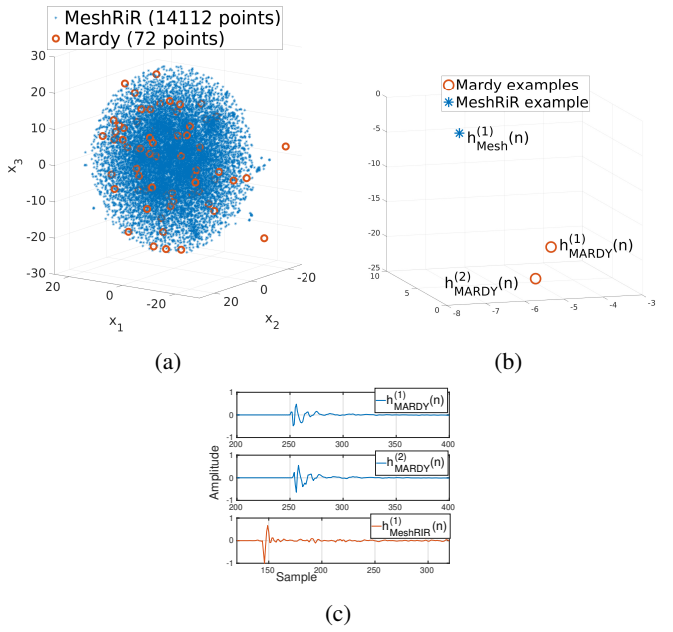

(a) (b) (c)

Fig. 2: t-SNE representation (a) cluster visualization of MARDY (orange circle) and MeshRiR (blue asterisk) (b) response cluster examples, (c) responses corresponding to (b)

F. Bayesian Optimization

Bayesian optimization [39] is a global hyperparameter optimization technique, constrained on the bounds of the hyperparameters, and is best suited for optimization with 20 or fewer hyper-parameters. The technique builds a surrogate function for the objective and quantifies the uncertainty in that surrogate using Gaussian process regression. Additionally, several parameters are required for initialization, including the type of acquisition function which guides the sampling for the optimal hyper-parameters [40]. Recent advancements can be found in [41]. In our optimization we set 11-hyperparameters: (i) duration P, and (ii) right circular shifts M_i $(i = 1,\ldots,10)$.

III. Bayesian Optimization of Stimuli Parameters

For Bayesian optimization, a "training" dataset of size TR is created with 11-channel combinations of room impulse responses from the MARDY and MESHRiR databases. The responses are input to a Bayesian optimization process that optimizes the duration and inter-channel shifts by minimizing a metric $\bar{\psi}_{SD}^{\text{bayes}}$, where

$$\bar{\psi}_{SD}^{\text{bayes}} = \frac{1}{R}\sum_{k=1}^{R}\sqrt{\frac{1}{11}\sum_{j=1}^{11}\|\hat{\mathbf{h}}_j^{(k)} - \mathbf{h}_j^{(k)}\|_2^2} \tag{6}$$

is the root-mean-square error (RMSE) averaged over the training set of size $R = TR$. The box constraints for the search for the optimal duration and circular shifts during the Bayesian optimization process are $\{P_{low}, P_{up}\}$ samples and $\{M_{i,low}, M_{i,up}\}$ samples, respectively. Algorithm 1 is used for the optimization of the 11-channel stimuli hyper-parameters, duration $(\hat{P})$ and circular shift $(\hat{M}_i; i = 1,\ldots,10)$, where the stimuli construction during each Bayesian optimization evaluation is given in (4).

Algorithm 1: Bayesian Optimization (BO) for Hyperparameter Search for Stimuli

Result: Stimuli(P^*, M_i^*), $i = 1,\ldots,10$; minimum : $\bar{\psi}_{SD}^{\text{bayes}}$

Initialize *bayesopt*: Construct base stimuli $\mathbf{x}_1(n)$ (Eq. 4), Gaussian Process Active Set Size=*GPA*, Number of Seed Points=*NP*, Exploration Ratio=*ER*, box constraints $\{P_{low}, P_{up}\}$ samples and $\{M_{i,low}, M_{i,up}\}$ samples, TR, and true MARDY and MESHRiR responses $\mathbf{h}_j^{(k)}$; $j = 1,\ldots,11; k = 1,2,\ldots,TR$;

while *maxTime* $\leq T$ *seconds* **do**

  For each $\hat{P}$ and $\hat{M}_i$ candidate, construct 11-channel stimuli using (4);

  Compute the convolution sum (3) using true responses and excitation stimuli with candidate $\hat{P}$ and $\hat{M}_i$;

  Estimate the responses using (5);

  Update hyperparameters $(\hat{P}, \hat{M}_i)$ using *bayesopt* to minimize $\bar{\psi}_{SD}^{\text{bayes}}$ using (6);

end

$T_{\text{stimuli}}^* = P^*/48000$ (seconds);

IV. Results

For *each* stimuli, the box-constraints during the optimization for the duration and circular shift were set empirically as $\{P_{low}, P_{up}\} = \{5, 30\} \times 48000$ (samples)[7], $\{M_{i,low}, M_{i,up}\} = \{4096, 131072\}; \forall i$ (samples). Additionally, GPA[8] $= 100$, ER[9] $= 0.5$ [38], NP[10] $= 10$, and $T = 259,200$ (s). The training set size is $TR = 500$, and the test set is of size $TS = 1000$, where each sample comprises 11 randomized responses per the dataset creation approach described in Sec. III.

A. Objective Results

As shown in Table I the shortest duration stimuli is log-sweep yields the smallest training set RMSE $\bar{\psi}_{SD}^{*,\text{log-sweep}} = 6.775 \times 10^{-6}$, whereas the RMSE for multitone-pink is $\bar{\psi}_{SD}^{*,\text{multitone-pink}} = 9.3592 \times 10^{-5}$, and the MLS $\bar{\psi}_{SD}^{*,\text{MLS}} = 8.943 \times 10^{-5}$. Also shown in Table I are the individual channel optimal right circular-shift value M_i (relative to channel 1) for each stimulus. The MLS and multitone-pink durations are similar. The advantage of a short duration stimuli includes a lower probability of insertion of impulsive noise during excitation. The present paper does not address immunity to steady-state noise (immunity which may be achieved using

[7] Based on footnote 3, the T_{stimuli} is box-constrained $\{5, 30\}$ (seconds)

[8] Fit Gaussian Process model to GPActiveSetSize or fewer points (using few points leads to faster GP model fitting, at the expense of possibly less accurate fitting)

[9] Parameter that balances between exploration and expolitation during global function optimization

[10] Number of initial evaluation points, specified as a positive integer, wherein bayesopt chooses these points randomly within the variable bounds

stimuli averaging). The generalization ability for each of the optimized stimuli is shown in Fig. 3 for the test set of size $TS = 1000$ where the y-axis is the averaged RMSE (computed using (6) with $R = TS$), with the 95% confidence interval of the mean, and expressed in dB. A log-sweep with random shift M_i and with $P_{\text{rand-sweep}} = P^*_{\text{log-sweep}} = 5.2379$ (s) result is also shown in Fig. 3 with the worst performance compared to the optimized stimuli. The best objective performance is achieved using the log-sweep stimuli with marginal differences in the 95% confidence interval ($\Delta_{\text{CI,log}} = 1.16$ dB, compared with $\Delta_{\text{CI,multi}} = 0.58$ dB, $\Delta_{\text{MLS,CI}} = 0.46$ dB, $\Delta_{\text{rand-sweep,CI}} = 0.43$ dB).

TABLE I: Bayesian optimized parameters for stimuli

Parameter	log-sweep	multitone-pink	MLS
T^*_{stimuli}	5.2379 (s)	28 (s)	21.845 (s)
M^*_1 (samples)	53886	78924	24308
M^*_2 (samples)	85006	48686	85296
M^*_3 (samples)	53256	64758	118423
M^*_4 (samples)	89316	66214	46918
M^*_5 (samples)	101774	83749	69150
M^*_6 (samples)	78699	109905	130623
M^*_7 (samples)	61029	6280	14266
M^*_8 (samples)	92437	103992	10699
M^*_9 (samples)	44056	55934	46022
M^*_{10} (samples)	18460	7271	5154

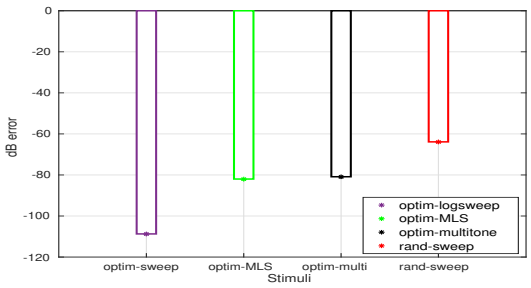

Fig. 3: Results from statistical analysis on $e^{\text{test-set}}_{\text{dB}}$.

B. Subjective Results

A listening experiment comprised two sessions in a standard-compliant listening room [4],[42] equipped with 11 loudspeakers (cf. Fig. 4(a)) and reference volume set to 72 dBC. In Session 1, a preference test for sound quality elicited responses from 18 participants by directly comparing 5-second extracts *between the three optimized stimuli whose values are given in Table I*. The participants rated the pleasantness of the sound on a continuous scale ranging from 0 (Very unpleasant) to 100 (Very pleasant). In Session 2, each of the 18 subjects participated in a single-trial forced choice test comprising the three full-duration optimized stimuli. The subjects then selected a preferred stimulus for performing an 11-channel measurement in their home. The second test measured the listeners' response to timbre **and** duration. The second session did not allow the subjects to switch, forcing them to listen


(a)

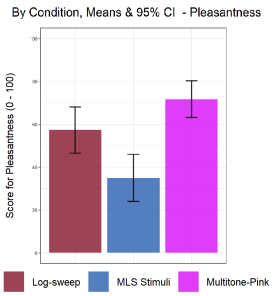

(b)

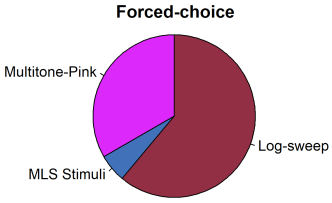

(c)

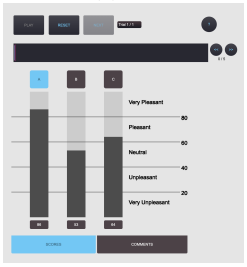

(d)

Fig. 4: (a) Reference room, results of (b) session 1 and (c) session 2, (d) test interface.

to the different duration stimuli to judge which stimuli they prefer for their in-room setup. Comments elicited from the subjects indicated that from the eleven listeners who preferred log sweep, nine preferred the timbre of multitone-pink but favored the shorter measurement time of log-sweep. The test subjects were aware of the need for repeated measurements in case of an unsuccessful deconvolution (e.g., due to impulsive noise). A statistically significant effect of the stimulus type on ratings was found for Session 1 using ANOVA. The multitone-pink signal was preferred by most assessors and scored on average higher than other stimuli. Post-hoc paired comparisons revealed that MLS scored significantly lower than the other two stimuli, but pink noise and log-sweep were statistically tied. In Session 2, the log-sweep was generally preferred by the panel, selected by 61.1% of assessors against 33.3% for the pink noise. Demo clips (HRTF downmix) are at https://github.com/SunilGBharitkar/ICASSP2023.

V. Conclusions & Future Directions

This paper presents results comparing three widely-used stimuli for simultaneously exciting and deconvolving room responses. Each stimulus is optimized using Bayesian techniques for their duration and circular shift amounts over a training dataset for an ITU 11-channel setup. The dataset is formed by augmenting the MARDY and MeshRiR databases creating a large corpus of 11-channel combinations. The objective performance demonstrates that log-sweep is the best candidate among the three stimuli. Furthermore, given the shorter duration of the log sweep, it is preferred for in-home room measurements. Future directions include robustness to impulsive noise and comparisons with PSEQ [27] and [28].

REFERENCES

[1] S. Bharitkar, "Deconvolution of room impulse responses from simultaneous excitation of loudspeakers," *Proc. 151st Audio Eng. Soc. Conv.,*, Online, Oct. 2021.

[2] R. Banka and S. Bharitkar, "Validation results of deconvolution of room impulse responses from simultaneous excitation of loudspeakers," *Proc. 153rd Audio Eng. Soc. Conv.,*, NY (USA), Oct. 2022.

[3] S. Bharitkar, "Bayesian Optimization for Simultaneous Deconvolution of Room Impulse Responses," *Proc. 36th IEEE Wkshp. Sig. Proc. Syst.*, Rennes (France), Nov. 2022.

[4] ITU-R BS. 2051-1, *Advanced sound system for programme production*, Int. Telecom. Union (ITU), 2018.

[5] S. Bharitkar and C. Kyriakakis, *Immersive Audio Signal Processing*, Springer-Verlag, June 2006.

[6] A. Carini, S. Cecchi, F. Piazza, I. Omiciuolo, G. Sicuranza,"Multiple position room response equalization in frequency domain," *IEEE Trans. Audio, Speech & Lang. Proc.*, 20(1), Jan. 2012, pp. 122–135.

[7] R. Mazur, F. Katzberg, A. Mertins,"Robust room equalization using sparse sound-field reconstruction," *2019 IEEE Int. Conf. Acoust., Speech & Sig. Proc.* (ICASSP 2019), Brighton (UK), April, 2019.

[8] M. Kolundžija, C. Faller, M. Vetterli,"Multi-channel low-frequency room equalization using perceptually motivated constrained optimization," *2012 IEEE Int. Conf. Acoust., Speech & Sig. Proc.* (ICASSP 2012), Kyoto (Japan), 2012.

[9] M. Schneider and W. Kellermann, "Adaptive listening room equalization using a scalable filtering structure in the wave domain," *2012 IEEE Int. Conf. Acoust., Speech & Sig. Proc.* (ICASSP 2012), Kyoto (Japan), 2012.

[10] D. Menzies, P. Coleman, F. Fazi, "A room compensation method by modification of reverberant audio objects," *IEEE/ACM Transactions on Audio, Speech, and Language Processing*, 29, Nov. 2020, pp. 239–252.

[11] J. Jungmann, R. Mazur, A. Mertins, "Joint time- and frequency-domain reshaping of room impulse responses," *2015 IEEE Int. Conf. Acoust., Speech & Sig. Proc.* (ICASSP 2015), Brisbane (Australia), 2015.

[12] S. Cecchi, A. Carini and S. Spors, "Room Response Equalization—A Review," *Applied Sciences*, 8(16), 2018.

[13] L. Fielder, "Practical Limits for Room Equalization," *Proc. 111th AES Conv.,*, NeY (USA), 2001.

[14] S. Bharitkar, C. Robinson, and A. Poulain, "Equalization of Spectral Dips Using Detection Thresholds," *Proc. 140th AES Conv.*, Paris (France), June 2016.

[15] C. Faller, "Modifying Audio Signals for Reproduction with Reduced Room Effect," *Proc. 147th AES Conv.*, NY (USA), Oct. 2019.

[16] D. Yellin and B. Friedlander, "Multichannel system identification and deconvolution: performance bounds," *IEEE Trans. Sig. Proc.* 47(5), 1999, pp. 1410–1414.

[17] T. Dobrowiecki, J. Schoukens, and P. Guillaume, "Optimized Excitation Signals for MIMO Frequency Response Function Measurements," *Proc. IEEE Instr. Meas. Tech. Conf.*,2005, pp. 1872-1877.

[18] F. Toole and S. E. Olive, "The Modification of Timbre by Resonances: Perception and Measurement," *J. Audio Eng. Soc.*, 36, 1988, pp. 122–142.

[19] ST 2095-1:2015, SMPTE Standard - Calibration Reference Wideband Digital Pink Noise Signal, Nov. 30, 2015.

[20] Y. Huang, J. Benesty. and J. Chen, "Identification of acoustic MIMO systems: Challenges and opportunities," *Sig. Proc.*, 86, 2006, pp. 1278–1295.

[21] G-B. Stan, J-J. Embrechts, and D. Archambeau, "Comparison of different impulse response measurement techniques," *J. Audio Eng. Soc.*, 50(4), April 2002, pp. 249–262.

[22] K. Prawda, S. J. Schlecht, and V. Valimaki, "Robust selection of clean swept-sine measurements in non-stationary noise," *J. Acoust. Soc. Amer.*, 151(3), March 2002, pp. 2117–2126.

[23] P. Majdak, P. Balazs, and B. Laback, "Multiple Exponential Sweep Method for Fast Measurement of Head-related Transfer Functions," *J. Audio Eng. Soc.*, 55(7/8), July/Aug. 2007, pp. 623–637.

[24] S. Weinzierl, A. Giese, and A. Lindau, "Generalized multiple sweep measurement," *Proc. 126th AES Conv.*, Munich (Germany), May 2009.

[25] C. Antweiler, A. Telle, and P. Vary, "NLMS-type system identification of MISO systems with shifted perfect sequences," *Proc. IWAENC*, Seattle (USA), 2008.

[26] C. Antweiler, S. Kuhl, B. Sauert, and P. Vary, "System identification with perfect sequence excitation-efficient NLMS vs. inverse cyclic convolution," *Proc. 11th ITG Conf. Speech Comm.*, Erlangen (Germany), 2014.

[27] C. Antweiler, A. Telle, P. Vary, and G. Enzner, "Perfect-sweep NLMS for time-variant acoustic system identification," *Proc. Int. Conf. Acoust. Speech Sig. Proc.* (ICASSP), Kyoto (Japan), 2012.

[28] Y. Nakahara, Y. Iiyama, Y. Ikeda, and Y. Kaneda, "Shortest impulse response measurement signal that realizes constant normalized noise power in all frequency bands," *J. Audio Eng. Soc.*, 70(1/2), Jan. 2022, pp. 24–35.

[29] I. F'ellejero, M. Zivanovic, I. Pmoabarren, A. Carlosena, "Application of multitone signals in room acoustics measurements," *Proc. IEEE Instr. & Meas. Tech. Conf.*, Budapest (Hungary), May 2001.

[30] J. Schoukens, R. Pintelon, "Identification of linear systems," *Pergamon Press*, 1991.

[31] E. Czerwinski, A. Voishvillo, S. Alexandrov, and A. Terekhov, "Multitone testing of sound system components–some results and conclusions, Pat 1: History and theory," *J. Audio Eng. Soc.*, 49(11), Nov. 2001, pp. 1011–1048.

[32] A. Potchinkov, "Low-crest-factor multitone test signals for audio testing," *J. Audio Eng. Soc.*, 50(9), Sept. 2002, pp. 681–694.

[33] J. Vanderkooy, "Aspects of MLS Measuring Systems," *J. Audio Eng. Soc.*, 42(4), April 1994, pp. 503–516.

[34] A. Farina, "Simultaneous Measurement of Impulse Response and Distortion with a Swept-Sine Technique," *Proc. 108th Audio Eng. Soc. (AES) Conv.*, Paris (France), Feb. 2000.

[35] J. Wen, N. Gaubitch, E. Habets, T. Myatt, and P. Naylor, "Evaluation of speech dereverberation algorithms using the MARDY database," *Proc. IWAENC*, Paris (France), Sept. 2006.

[36] S. Koyama, T. Nishida, K. Kimura, T. Abe, N. Ueno, and J. Brunnstrom, "MeshRIR: A dataset of room impulse responses on meshed grid points for evaluating sound field analysis and synthesis methods," *Proc. IEEE-WASPAA*, Mohonk, NY (USA), 2021.

[37] L. van der Maaten, and G. Hinton, "Visualizing Data using t-SNE," *J. Mach. Learn. Res.*, vol. 9, 2008, pp. 2579–2605.

[38] G. De Ath, R. M. Everson, A. Rahat, and J. E. Fieldsend, "Greed is Good: Exploration and Exploitation Trade-offs in Bayesian Optimisation," *ACM Trans. Evol. Learn. Optim.*, 1(1), March 2021, pp. 1–22.

[39] J. Snoek, H. Larochelle, and R. Adams, "Practical Bayesian optimization of machine learning algorithms," *Proc. Neural Inf. Proc. Syst. (NIPS)*, 2012.

[40] P. I. Frazier, "A tutorial on Bayesian optimization," *arXiv:1807.02811v1*[stat.ML], July, 2018.

[41] J. R. Doppa, V. Aglietti, and J. Gardner, "Advances in Bayesian Optimization," *Neural Inf. Proc. Syst. (NIPS) Wkshp.*, Dec. 2022.

[42] ITU-R BS. 1116, *Methods for the subjective assessment of small impairments in audio systems*, Int. Telecom. Union (ITU), 2015.